

INVESTIGATION OF TI-6AL-4V ALLOY RESPONSE TO ATMOSPHERIC  
RE-ENTRY EXPOSURE

JESSICA LYNN BUCKNER

Doctoral Program in Materials, Science, and Engineering

APPROVED:

\_\_\_\_\_  
Stephen Stafford, Ph.D., Chair

\_\_\_\_\_  
David Roberson, Ph.D.

\_\_\_\_\_  
Stella Quinones, Ph.D.

\_\_\_\_\_  
Russell Chianelli, Ph.D.

\_\_\_\_\_  
Charles Ambler, Ph.D.  
Dean of the Graduate School

PREVIEW

Copyright ©

by

Jessica Lynn Buckner

2016

## **Dedication**

For my parents and brother.

PREVIEW

# INVESTIGATION INTO TI-6AL-4V ALLOY RESPONSE TO ATMOSPHERIC RE-ENTRY EXPOSURE

by

JESSICA LYNN BUCKNER, B.S. Metallurgical and Materials Engineering

DISSERTATION

Presented to the Faculty of the Graduate School of  
The University of Texas at El Paso  
in Partial Fulfillment  
of the Requirements  
for the Degree of

DOCTOR OF PHILOSOPHY

Department of Metallurgical, Materials, and Biomedical Engineering

THE UNIVERSITY OF TEXAS AT EL PASO

December 2016

ProQuest Number: 10239940

All rights reserved

INFORMATION TO ALL USERS

The quality of this reproduction is dependent upon the quality of the copy submitted.

In the unlikely event that the author did not send a complete manuscript and there are missing pages, these will be noted. Also, if material had to be removed, a note will indicate the deletion.



ProQuest 10239940

Published by ProQuest LLC (2017). Copyright of the Dissertation is held by the Author.

All rights reserved.

This work is protected against unauthorized copying under Title 17, United States Code  
Microform Edition © ProQuest LLC.

ProQuest LLC.  
789 East Eisenhower Parkway  
P.O. Box 1346  
Ann Arbor, MI 48106 – 1346

## Acknowledgements

It has been my honor to work with Dr. Stephen Stafford as my dissertation chair as I progressed through my research. His patience, input, and support have been a huge part of my success, and I cannot thank him enough. His expertise in titanium and failure analysis were instrumental during my tenure at UTEP, on par with his kind words and welcoming nature. I would also like to thank John “Danny” Olivas for bringing this exciting work to UTEP, and reminding me to always “lean forward”. Darren Cone contributed tremendously to this work, sharing his knowledge of materials and space conditions, and acting as a technical review through the stages of my research and writing. I would like to thank him for the countless hours spent in meetings and always maintaining an open door policy, which led me to many “a-ha” moments. I would like to thank Dr. Roberson, Dr. Quinones, and Dr. Chianelli for serving on my committee. I would like to acknowledge the Metallurgical, Materials, and Biomedical Engineering (MMBME) Department, which I have called home for the past several years, for their support and guidance. I would like to thank the MMBME department, the SMART grant sponsored through the American Society for Engineering Education (ASEE), the Center for Advancement of Space Safety and Mission Assurance Research (CASSMAR), and the various private organizations that provided funding and financial support for tuition, research, and conferences. Thank you to the Herrera, Stafford, and Associates (HSA) team for assistance with laboratory services. I would also like to acknowledge Mike Ciannilli and Rick Russell at Kennedy Space Center who provided support and access to *Columbia* artifacts.

Personally, I would like to thank my parents and older brother for always teaching me that education was important and to always fight for my goals. Last but not least, I would like to thank my husband, who has supported me and lifted me up, even when I was at my wits end. It was with his understanding and support that I pushed past a masters and completed a Ph.D.

## Abstract

Ti-6Al-4V is a widely used aerospace alloy for its high strength-to-weight ratio and high operating temperature properties. Despite widespread use, titanium and its alloys have been shown to ignite in oxygen and nitrogen rich test streams. The reactivity of titanium is attributed to the high solubility for oxygen that increases with temperature, accelerating the oxidation rate and resulting in a combustion reaction. When introduced to the monatomic oxygen rich and high enthalpy re-entry environment, Ti-6Al-4V X-link components from the space shuttle *Columbia* exhibited accelerated oxidation and combustion behavior. Ti-6Al-4V metal plates tested in the simulated re-entry environment of an arc-jet facility have also exhibited ignition and combustion responses. A forensic material characterization study of the X-links and arc-jet samples is necessary to gain a better understanding of the material response in the dynamic and extreme environment of re-entry.

Materials characterization methods, in the form of microstructural analysis, scanning electron microscopy, energy dispersive X-ray spectroscopy, X-ray diffraction, and microhardness testing, are used to identify the current state of the degraded Ti-6Al-4V material and glean knowledge about the alloy response during re-entry. Data from X-link components is compared to the Ti-6Al-4V samples previously tested in the simulated re-entry arc-jet facility conditions. Several similarities in microstructural features and oxide compound detection suggest that qualitative and quantitative conclusions can be drawn from comparison of actual and simulated re-entry conditions. Furthermore, subtleties between oxidation, ignition, and combustion reaction thresholds were identified. A thorough materials characterization of these materials will yield insight into the discrimination between different material responses of titanium alloys. Widespread use of titanium alloys in space vehicles warrants a thorough characterization of their potential failure modes to help ensure the safe and reliable operation of future spaceflight vehicles.



## Table of Contents

Acknowledgements .....	v
Abstract .....	vi
Table of Contents .....	vii
List of Tables .....	ix
List of Figures .....	x
Chapter 1: Introduction and Presented Published Papers .....	1
1.1 Background .....	1
1.2 Justification .....	5
1.3 Published Works .....	7
Chapter 2: Literature Review .....	10
2.1 Characteristics of Ti-6Al-4V .....	10
2.2 Oxidation of Titanium .....	15
2.3 Ignition and combustion of Titanium .....	18
2.4 Particulate Combustion of Titanium .....	26
Chapter 3: Experimental Methods .....	31
3.1 Primary Sectioning of X-links .....	31
3.2 Secondary Sectioning of X-links .....	32
3.3 Sectioning of arc-jet samples .....	34
6.1.1 Arc-jet Supplementary Data .....	35
3.4 Heat Treatment Study .....	39
Chapter 4: Materials Characterization of the Oxidation and Combustion Behavior of Ti-6Al-4V X-links from the Space Shuttle <i>Columbia</i> .....	40
4.1 Introduction .....	40
4.2 Methods .....	43
4.3 Results and Discussion .....	43
4.4 Conclusions .....	53
4.5 Acknowledgements .....	54

Chapter 5: Investigation into the response of Ti-6Al-4V alloy to atmospheric	
re-entry exposure .....	55
5.1 Introduction .....	55
5.2 Methods .....	59
5.3 Results .....	61
5.4 Conclusions .....	78
5.5 Acknowledgements .....	80
Chapter 6: Results and Discussion .....	81
6.1 X-link Results .....	81
6.2 Arc-jet Results .....	96
Chapter 7: Heat Treatment Study Results .....	109
7.1. Microstructural Features .....	110
7.2 Microhardness Testing .....	113
7.3 Summary/Findings .....	115
Chapter 8: Conclusions .....	116
8.1 Summary and Conclusions .....	116
8.2 Recommendations and Future Work .....	123
References .....	125
Appendix A .....	131
Appendix B .....	133
Vita .....	135

## List of Tables

Table 2.1. Properties of Ti-6Al-4V as they relate to combustion. Data for pure titanium retrieved from [23], Ti-6Al-4V from [9].....	14
Table 2.2. Physical properties of common titanium oxides. Data retrieved from matweb.com...	17
Table 2.3. Ignition temperatures of bulk Ti and Ti alloys. ....	25
Table 3.1. Test matrix for chosen samples. ....	35
Table 5.1. Nomenclature of samples discussed in paper. ....	60
Table 5.2. Average microhardness and population standard deviation for samples 1-4. ....	78
Table 6.1. Locations of data discussion of X-link and arc-jet samples in dissertation.....	81
Table 6.2. Averages microhardness values and population standard deviation for sections D.2, E.2, and G.1. ....	96
Table 7.1. Test matrix for heat treatment study. ....	110

## List of Figures

Figure 1.1. Schematic of configuration of X-links within the shuttle. Adapted from [3].	3
Figure 1.2. Top view as-received photographic documentation of the recovered X-links.	3
Figure 1.3. The three different classifications of material response observed in arc-jet testing.	4
Figure 1.4. Arc-jet classifications of material response as they relate to enthalpy and dynamic pressure. Adapted from [7].	5
Figure 2.1. Illustration of the HCP $\alpha$ and BCC $\beta$ unit cells. Adapted from [20].	13
Figure 2.2. The pseudo-binary phase diagram of Ti-6%Al with additions of vanadium. Vertical line corresponds to a composition of Ti-6%Al-4%V, indicating approximate $\beta$ -transus temperature of 1950°F. Adapted from [21].	13
Figure 2.3. Microstructure of two-phase Ti-6Al-4V alloy: a) martensitic, b) globular, c) necklace, d) lamellar, e) bimodal. Adapted from [22].	14
Figure 2.4. The titanium rich portion of the titanium-oxygen phase diagram. Adapted from [32].	17
Figure 2.5. The titanium rich portion of the titanium-nitrogen phase diagram. Adapted from [33].	18
Figure 3.1. Primary sectioning of port (a) and starboard (b) X-links, top view.	32
Figure 3.2. High resolution images of starboard pieces D (a), E (b), and G (c).	33
Figure 3.3. High resolution images of arc-jet specimens 8 (a), 16 (b), 17 (c), and 28 (d).	35
Figure 3.4. Test article configuration schematic. Adapted from [7].	36
Figure 3.5. Insertion time vs. sample temperature data for Run 1806, Specimen 8. Adapted from data files from [7].	37
Figure 3.6. Insertion time vs. sample temperature data for Run 1808, Specimen 16. Adapted from data files from [7].	37
Figure 3.7. Insertion time vs. sample temperature data for Run 1811, Specimen 17. Adapted from data files from [7].	38
Figure 3.8. Insertion time vs. sample temperature data for Run 1813, Specimen 28. Adapted from data files from [7].	38
Figure 4.1. The X-links as recovered, top view, with box indicating burn through in the flange. From [3].	41
Figure 4.2. Top view of Regions A (left) and B (right).	43
Figure 4.3. a) Secondary electron image of blue-tinted region with boxed area indicating EDS scan area; b) EDS spectrum obtained from the blue-tinted region	44
Figure 4.4. Inboard (a) and outboard (b) microstructures. Kroll's reagent.	45
Figure 4.5. a) Optical image of deposition layer (Kroll's); and, b) Backscattered electron image of deposition layering in Region A (boxes indicating selected areas for EDS spot analysis).	47
Figure 4.6. EDS spectra from a) Scan One, and b) Scan Two from Region A.	48
Figure 4.7. a) Secondary electron image of porous surfaces resembling shrinkage porosity from surface, top surface and b) Secondary electron image of porosity, top surface.	49
Figure 4.8. Inboard (a) and outboard (b) microstructures from Region B. Kroll's reagent.	51
Figure 4.9. Backscattered electron image of outboard deposit (b), with higher magnification image of porous layer surrounding the large inclusion particles.	52
Figure 4.10. EDS spectra from a) Scan One, and b) Scan Two from Region B.	53

Figure 5.1. As-received photographic documentation of the port and starboard X-links.....	59
Figure 5.2. The three different classifications of material response observed from arc-jet testing. .....	59
Figure 5.3. Starboard X-link region of interest with numbered sections.....	60
Figure 5.4. Class II (a) and Class III (b) arc-jet samples. ....	60
Figure 5.5. Complementary microstructures through thickest section of port (a) and starboard (b) X-links.....	65
Figure 5.6. Initial microstructural state of the arc-jet samples. ....	66
Figure 5.7. Forward facing flow microstructures for starboard X-link section 1 (a), starboard X- link section 2 (b), arc-jet sample Class II (c), and arc-jet sample Class III (d). ....	68
Figure 5.8. Back facing flow microstructures for starboard X-link section 1 (a), starboard X-link section 2 (b), arc-jet sample Class II (c), and arc-jet sample Class III (d).....	70
Figure 5.9. Backscattered electron images of granular features coalescing to form a solid layer in X-link sample 2 (a) and arc-jet sample 3 (b). ....	72
Figure 5.10. EDS spectrum of granular features in X-link sample 1 (a) and arc-jet sample 3 (b). .....	73
Figure 5.11. X-ray diffraction patterns for the less thermally degraded X-link sample 2 and arc- jet sample 3 (a) and the more thermally degraded X-link sample 1 and arc-jet sample 4 (b). ....	75
.....	77
Figure 5.12. Microhardness values traversing from forward to back facing flow side for samples 1 and 2 (a) and samples 3 and 4 (b). ....	77
Figure 6.1. Secondary sectioning of section E.....	82
Figure 6.2. Secondary sectioning of section G. ....	83
Figure 6.3. Microstructure of section E.3, showing martensitic $\alpha$ within large prior $\beta$ grains. ...	84
Figure 6.4. Microstructural features of section G.1 at the inboard (a) and outboard (b) sides. ....	86
Figure 6.5. Microstructure of the Ti-6Al-4V material at the titanium/MP35N fastener interface. .....	87
Figure 6.6. Backscattered electron image of silicon rich embedded particle in section E.3 (a) and EDS spectrum of boxed area (b). ....	88
Figure 6.7. Backscattered electron image of section G.1 inboard side deposit (a), with white boxed area indicating location of zoomed image in (b). Black boxes indicate locations of EDS scans. ....	90
Figure 6.8. EDS spectra of section G.1 for box 1, porous material in Figure 6.7a (a) and box 2, granular features in Figure 6.7b (b). ....	91
Figure 6.9. Location of XRD data collection (a) and diffraction patterns for section E.2 (b). ....	92
Figure 6.10. Diffraction pattern for section E.3. ....	93
Figure 6.11. Diffraction patterns for the inboard (bottom) and outboard (top) side of section G.1. .....	94
Figure 6.12. Traversing microhardness testing results for sections D.2, E.2, and G.1 .....	95
Figure 6.13. Microstructural features of the leading edge (a) and trailing edge (b) of Class II arc- jet specimen 16. ....	97
Figure 6.14. Microstructural features of the leading edge (a) and trailing edge (b) of Class III arc- jet specimen 28. ....	98
Figure 6.15. Backscattered electron microscope images of Class II arc-jet specimen 16, with close-up of (a) in (b). ....	100

Figure 6.16. EDS spectra of Class II arc-jet specimen 16 with box 1, intergranular deposit (a) and box 2, granular features (b) in Figure 6.15b.....	101
Figure 6.17. Backscattered electron microscope images of Class II arc-jet specimen 17, with arrow in (a) indicating location of (b).....	103
Figure 6.18. . EDS spectra of Class II arc-jet specimen 17 with box 1, star-like features (a) and box 2, granular features (b) in Figure 6.15b. ....	104
Figure 6.19. Backscattered electron image of star-like morphology (a) granular features in both (a) and (b) in Class III arc-jet specimen 28.....	105
Figure 6.20. EDS spectra for Class III arc-jet specimen 28 of box 1, star-like solidification features in Figure 6.5a (a) and box 2, granular top layer in Figure 6.5b (b).....	106
Figure 6.21. Diffraction patterns for Class II arc-jet specimens 8 and 16. ....	107
Figure 6.22. Diffraction patterns Class III arc-jet specimens 17 and 28. ....	108
Figure 7.1. Microstructural features of samples in heat treatment study.....	113
Figure 7.2. Average microhardness readings of the heat treated samples. ....	114
Figure 7.3. Plot showing average microhardness readings versus low and high reading from the two samples analyzed per heat treatment.....	115
Figure 8.1. Suggested temperature map of the X-links based on microstructural features observed at the inboard side. ....	118
Figure 8.2. Suggested temperature map of the X-links based on microstructural features observed at the outboard side. ....	119

## Chapter 1: Introduction and Presented Published Papers

### 1.1 BACKGROUND

On February 1<sup>st</sup>, 2003, NASA's Space Shuttle *Columbia* endured a catastrophic failure during re-entry into Earth's atmosphere. Ultimately, all seven crew members lost their lives in this tragic event. Root-cause analysis determined that a breach of the reinforced carbon-carbon (RCC) leading edge of the port wing was caused by a piece of insulating foam that detached from the external fuel tank during lift-off. This breach allowed superheated gas ingestion into the vehicle during re-entry, which ultimately degraded the substructural components and integrity of the space shuttle [1].

Following reconstruction of *Columbia*, evidence suggested that the widely used aerospace alloy, Ti-6Al-4V, exhibited an accelerated degradation believed to be caused by oxidation, ignition, and combustion reactions intensified by exposure to the monatomic oxygen rich, high enthalpy conditions of the re-entry environment. Scientific interest promoted the testing of Ti-6Al-4V plates in the simulated re-entry environment of the arc-jet. These experiments also demonstrated a propensity of Ti-6Al-4V to exhibit accelerated oxidation, ignition, and combustion behavior in extreme conditions. Little research into the material state and properties after exposure to these environments has been documented, thus a detailed materials characterization study was designed to better understand the complexities of material response. A forensic analysis of the material exposed to the actual re-entry environment *Columbia* endured and the simulated re-entry environment of the arc-jet is necessary to discriminate between specific re-entry conditions that can result in catastrophic material reactions and reduction in structural integrity of space vehicles.

#### 1.1.1 Environmental Conditions

The re-entry environment is a monatomic oxygen rich, low pressure, and high enthalpy environment. It is highly aggressive and dynamic. Exact temperature and pressure conditions of the re-entry environment are dependent on altitude. In terms of vertical temperature, there are

four atmospheric layers [2]. In order of increasing altitude are the troposphere, stratosphere, mesosphere, and thermosphere. Modeling results published in the *Columbia* Crew Survival Report by NASA indicate that breakup of *Columbia* occurred in the mesosphere, between 180-210 thousand feet altitude [3]. In the mesosphere, low temperatures prevail and molecular oxygen and nitrogen still compose 99% of the air, with virtually the same mixings as air at sea level (78% N<sub>2</sub>, 20.9% O<sub>2</sub>, 1.1% other) [2]. The high velocities produced by vehicle deceleration can result in the dissociation of molecular O<sub>2</sub> and N<sub>2</sub> gases, converting the species to their atomic forms. Atomic nitrogen and oxygen are more reactive than their molecular forms and produce a more aggressive environment in which oxidation and combustion are accelerated.

### **1.1.2 X-link Background**

The X-links, also known as crew module attachment fittings, are a substructural component composed of Ti-6Al-4V that connected the crew module, forward fuselage, and midbody structures of the vehicle in the longitudinal direction. There are two X-links, one each for the port and starboard side of the vehicle. Figure 1.1 illustrates the configuration of the X-links within the shuttle. The X-links were secured to the shuttle structures with fasteners made of MP35N, a nickel-cobalt-chromium-molybdenum alloy trademarked by SPS technologies. The top view of the as-received port and starboard X-links as configured within the shuttle are shown in Figure 1.2. Relative to the port X-link, the starboard X-link exhibited more mass loss, discoloration, and is missing the aft-most fastener. The fastener heads exhibit evidence of exposure to forward-to-aft flow conditions, while the webbing of both X-links contain evidence of exposure to aft-to-forward flow conditions. Structural debris analysis suggests that initial failure occurred immediately aft of the starboard X-link from a combination of structural loads and thermal degradation, and the vehicle proceeded to separate from starboard to port side [3]. Despite similar flow patterns, the starboard X-link was recovered in the forebody debris field and the port X-link in the midbody debris field; this physical separation is theorized to have occurred after the combustion event.



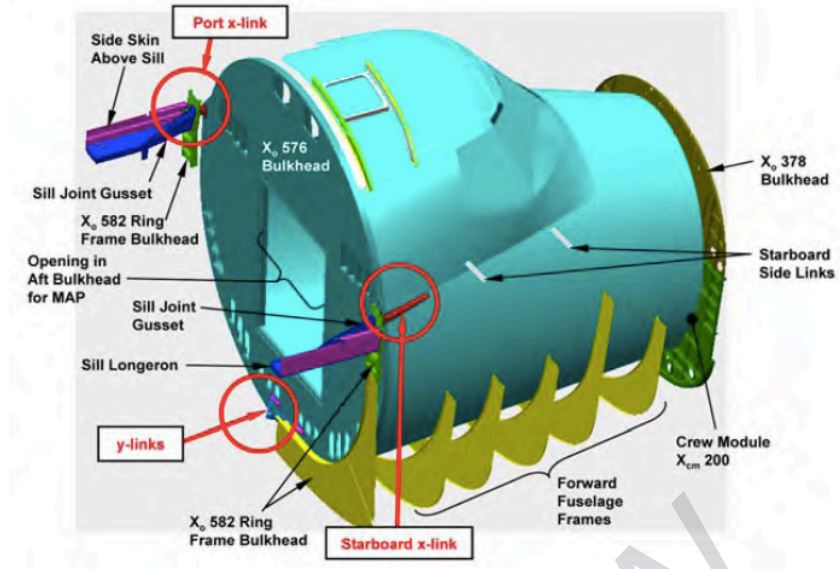


Figure 1.1. Schematic of configuration of X-links within the shuttle. Adapted from [3].



Figure 1.2. Top view as-received photographic documentation of the recovered X-links.

### 1.1.3 Arc-jet Testing Background

To better understand the physical features and history of the X-links, Ti-6Al-4V plates were tested in an arc-jet facility. Arc-jet testing currently represents the best ground-based simulation of a re-entry environment by providing the best ability to explore the oxidation behavior of materials under extreme conditions [4]. The arc-jet created the equivalent of a high altitude, hypersonic wind tunnel facility that heats and accelerates  $O_2$  and  $N_2$  gases through a nozzle and onto the surface of a sample [5]. Testing parameters, to include air content, angle of attack, and pressure, were designed to encompass conditions modeling predicted the X-links

were exposed to. Air content and angle of attack remained constant for all test specimens. Three different classifications of material response were observed from arc-jet testing (Figure 1.3). Class I represents material passivation, Class II represents ignition and initiation of melting without sustained combustion, and Class III represents ignition with sustained combustion. For explanation, Figure 1.4 shows where the classifications lie in a plot of inferred enthalpy versus dynamic pressure. The triangles indicated individual test samples. Note that higher dynamic pressure and inferred enthalpy contributed to a more aggressive environment and material reaction.

Testing was initially designed with a 30° angle of attack between incident air flow and metal plate, with the metal plate flush mounted on the stand. One sample was unknowingly installed with a slight protuberance from the mount. With this protuberance, and thus a higher effective ballistic number, ignition and combustion occurred. Without any protuberance, and thus a lower effective ballistic number, only oxidation with no ignition or combustion behavior was exhibited. The results of the arc-jet testing provided evidence that ignition and combustion are plausible phenomena for titanium alloys in the re-entry conditions the *Columbia* X-links were exposed to, though testing did not establish all conditions of re-entry supporting combustion.

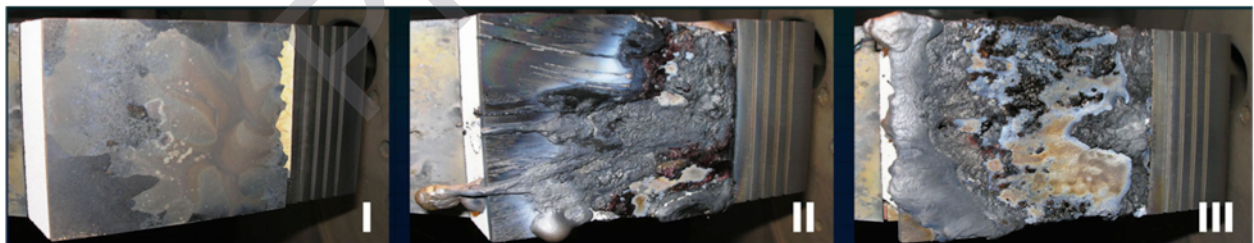


Figure 1.3. The three different classifications of material response observed in arc-jet testing.

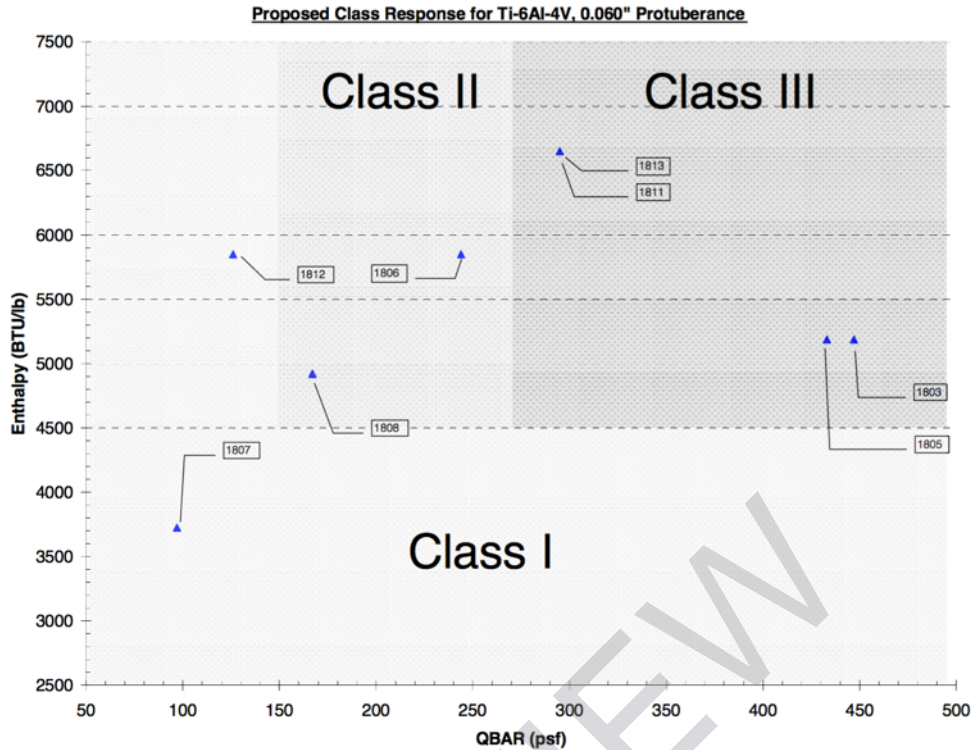


Figure 1.4. Arc-jet classifications of material response as they relate to enthalpy and dynamic pressure. Adapted from [6].

## 1.2 JUSTIFICATION

During accident reconstruction, NASA's Object Re-entry Survival Analysis Tool (ORSAT) predicted entry heating alone was not sufficient to explain the observed damage on the X-links, most notably the burn through in the flange area [3]. In order to cause the observed damage, analytical predictions from ORSAT estimated a required heat rate that was an order of magnitude higher than the maximum peak aero heating the vehicle could have experienced. These findings led to the consideration of other possible material interactions: shock-shock interaction and metal combustion. While it is understood that shock-shock interaction is a competing theory, the focus of this dissertation is on the latter. There are no shock-shock interactions in the arc-jet, and because the dissertation is a comparative analysis between arc-jet and actual re-entry conditions, shock- shock interaction is not considered.

During *Columbia* accident reconstruction, overhead windows from the forward fuselage were observed to contain a metallic deposit. This metallic ‘char’ layer was found to be largely composed of metal oxides, and an oxidized layer of Ti-6Al-4V was deposited prior to that of an aluminum alloy [7]. Simply from the standpoint of relative melting temperatures between aluminum and titanium alloys, and given the larger overall weight percentage of aluminum alloys comprising the shuttle construction, the observations from the overhead window char layer were puzzling. Thus, arc-jet testing was utilized in an attempt to explain these observations. As noted previously, Ti-6Al-4V exhibited three different material responses, with higher effective ballistic numbers producing more extreme material interactions. The complexity of the Ti-6Al-4V combustion reaction is demonstrated by the differing physical features of the X-links and arc-jet samples. Understanding the subtleties amongst oxidation, ignition, and combustion mechanisms of the alloy is instrumental in determining graceful degradation of titanium in the extreme environment of re-entry.

A forensic materials characterization study of two separate Ti-6Al-4V components that have been exposed to re-entry conditions, both actual and simulated, will further the understanding of bulk metal combustion in the extreme environment. Qualitative and quantitative correlations will be made between the X-links and the arc-jet samples in an effort to relate the known parameters of testing to the unknown parameters of the X-links re-entry into the atmosphere. This comparison will help to determine if ground-based testing methods are sufficiently representative of the actual environment to encompass conditions supportive of metal combustion. These results will also aid in differentiating separate material reactions in an effort to identify the mechanism of Ti-6Al-4V combustion in a re-entry environment.

Given the extensive use of titanium alloys as structural components in modern aerospace vehicles, consideration for the accelerated thermal degradation due to exposure of these alloys to the re-entry environment cannot be neglected. The aerospace community must be aware of a well-predicted degradation of materials being sent into space. It has been established that not every re-entry condition is supportive of combustion, but a catastrophic reaction has been

demonstrated as a very real possibility through arc-jet testing. Detailed materials characterization of the *Columbia* X-links and arc-jet samples will advance the understanding of titanium reactivity in the extreme environment of atmospheric re-entry.

This research is not applicable only to aerospace applications. Extreme environmental exposure is found in many industries, such as power generation and automotive [8]. The alloy is used extensively for the housings of turbine engines, a component of large proportions and complexity. Titanium alloys used in turbine engines have had occurrence of combustion [9]. Ti-6Al-4V is also used in the the automotive industry for special parts needing high temperature resistance. On air frames, Ti-6Al-4V is used as flow diverters, torque tubes for brakes, and helicopter rotor hubs. These extreme environments share many characteristics, namely high enthalpy and high flow conditions. Reliance on material integrity is paramount, and this research will aid in determining material reactions and characteristics in compromising environments.

### **1.3 PRESENTED WORKS**

Two chapters in this dissertation are composed of published and presented works. The citations and abstracts for each published work along with corresponding chapters are listed as follows:

#### ***Chapter 4***

The material in Chapter 4 was presented and published in the proceedings of the Materials, Science, and Technology (MS&T) 2015 conference, and is cited as follows:

J.L. Buckner, S.W. Stafford, D.M. Cone, “Materials Characterization of Ti-6Al-4V X-links from the Space Shuttle *Columbia*,” in Proceedings of MS&T 2015, Columbus, OH, October 4-8, 2015.

This work was a preliminary presentation of data gathered from materials characterization of two sections of *Columbia*. To supplement Chapter 4, further characterization of *Columbia* sections

will be discussed in Chapter 6. Permission to use the article cited above is documented in Appendix A.

### ***Abstract***

Recovered artifacts from the Space Shuttle *Columbia* provide a unique opportunity to examine a broad spectrum of materials exposed to the extreme environment of earth re-entry. The degradation states of these components offer a unique perspective into material behavior in this highly reactive environment. The crew module X-links, which are composed of Ti-6Al-4V and provided structural support to the crew module within the fuselage, exhibit evidence of both oxidation and combustion phenomena. The conditions supporting ignition and combustion of bulk metals are not fully understood, due to the many compounding factors affecting variable oxidation behavior of metals. Materials characterization of the *Columbia* X-links will yield further insight into the discrimination between the oxidation, ignition, and combustion response of titanium alloys. Widespread use of titanium alloys in space vehicles warrants a thorough characterization of their potential failure modes to help ensure the safe and reliable operation of future spaceflight vehicles.

### ***Chapter 5***

The material in Chapter 5 was presented and published in the proceedings of the International Association for Advancement of Space Safety (IAASS) 2016 conference, and is cited as follows:

J.L. Buckner, S.W. Stafford, D.M.Cone, J.D. Olivas, “Investigation of Ti-6Al-4V alloy response to atmospheric re-entry exposure,” in Proceedings of IAASS 2016, Melbourne, FL, May 18-20, 2016.

This paper serves as a comparison between arc-jet and X-link results. Supplementary X-link data is found in Chapter 6. Permission to use the material cited above is document in Appendix B.



## ***Abstract***

Ti-6Al-4V is a widely used aerospace alloy for its high strength-to-weight ratio and high operating temperature properties. Despite widespread use, titanium and its alloys have been shown to ignite in oxygen and nitrogen rich test streams. The reactivity of titanium is attributed to the high solubility for oxygen that increases with temperature, accelerating the oxidation rate and resulting in a combustion reaction. When introduced to the monatomic oxygen rich and high enthalpy re-entry environment, Ti-6Al-4V X-link components from the space shuttle *Columbia* exhibited accelerated oxidation and combustion behavior. Ti-6Al-4V metal plates tested in the simulated re-entry environment of an arc-jet facility have also exhibited ignition and combustion responses. A forensic material characterization study of the X-links and arc-jet samples is necessary to gain a better understanding of the material response in the dynamic and extreme environment of re-entry. Data from X-link components is compared to the Ti-6Al-4V samples previously tested in the simulated re-entry arc-jet facility conditions. The observation of similar microstructural and solidification features in conjunction with similar oxide compound detection suggest that arc-jet testing is representative of the re-entry environment effect on titanium and its alloys. A thorough materials characterization of these materials will yield insight into the discrimination between the oxidation, ignition, and combustion response of titanium alloys. Widespread use of titanium alloys in space vehicles warrants a thorough characterization of their potential failure modes to help ensure the safe and reliable operation of future spaceflight vehicles.

## Chapter 2: Literature Review

The titanium alloy, Ti-6Al-4V, is commonly utilized as a structural material for its attractive properties, to include high operating temperature capabilities and excellent corrosion resistance. Yet, research has shown that nearly every commercial titanium alloy can ignite [10] [11]. Despite a relatively mature understanding of combustion involving gaseous and liquid fuels, knowledge regarding combustion of bulk metals is not as extensive. This is likely due to the many compounding factors affecting oxidation and combustion that complicate analysis, to include purity, gas composition, pressure, velocity past the surface, state of subdivision, and previous processing [12]. Several accidents involving metal-oxygen combustion in the space program have indicated that this phenomena deserves further consideration [13-14]. This literature review presents characteristics of the base element titanium and its  $\alpha+\beta$  alloys as it relates to the oxidation, ignition, and combustion behavior. Ti-6Al-4V is not heavily alloyed, therefore several physical properties, oxide formation, and combustion mechanisms are similar to pure titanium metal.

### 2.1 CHARACTERISTICS OF Ti-6Al-4V

Ti-6Al-4V is a widely used aerospace alloy utilized for its high strength-to-weight ratio, corrosion resistance, and high operating temperature capabilities [15]. The microstructure is two phased, consisting of a Body Centered Cubic (BCC) beta ( $\beta$ ) and Hexagonal Close Packed (HCP) alpha ( $\alpha$ ) (Figure 2.1). The addition of aluminum stabilizes the  $\alpha$  phase, while the addition of vanadium stabilizes the  $\beta$  phase. Other  $\alpha$  stabilizers include oxygen and nitrogen. An important parameter in Ti-6Al-4V processing is the  $\beta$ -transus temperature, defined as the temperature above which only the  $\beta$  phase is present at equilibrium [16]. HCP  $\alpha$  exists below the  $\beta$ -transus, while BCC  $\beta$  exists above the  $\beta$ -transus. Figure 2.2 illustrates the pseudo-binary phase diagram of Ti-6%Al with additions of vanadium, indicating an approximate  $\beta$ -transus temperature of 1850°F-1950°F (1010°C-1065°C). The  $\beta$ -transus is dependent upon manufacturer, and literature widely disagrees on this value. Reference [16], focusing on heat